

# Search for Time-Reversal Violation in the Beta Decay of $^8\text{Li}$

M. Allet, W. Hajdas, J. Lang, H. Lüscher, R. Müller, O. Naviliat-Cuncic, and J. Sromicki  
*Institut für Mittelenergiephysik, Eidgenössische Technische Hochschule Zürich, CH-8093 Zürich, Switzerland*

A. Converse, W. Haeberli, M. A. Miller, and P. A. Quin

*University of Wisconsin, Madison, Wisconsin 53706*

(Received 5 August 1991)

The transverse polarization in a plane perpendicular to the nuclear spin has been measured for electrons emitted in the beta decay of polarized  $^8\text{Li}$  nuclei. The amplitude  $R$  of the time-reversal-violating triple correlation between nuclear spin, momentum, and spin of the electron has been determined. Our result,  $R = 0.004 \pm 0.014$ , is consistent with time-reversal invariance and provides a first direct limit on the imaginary charged weak tensor interaction  $-0.03 < \text{Im}(C_T + C_T')/C_A < 0.05$ .

PACS numbers: 23.40.Bw, 11.30.Er, 27.20.+n

Shortly after the conjecture by Yang and Lee [1] in 1956 that parity ( $P$ ) might be violated in some processes, experiments showed that this fundamental symmetry (along with charge conjugation  $C$ ) appears to be maximally broken in *all* transitions mediated by the weak interaction. The situation for time-reversal violation (TRV) is entirely different. Small effects of  $CP$  (or  $T$ ) violation [2] were first observed in neutral  $K$  meson decay by Christensen *et al.* in 1964.  $T$  violation has not been observed in *any other* system, despite numerous attempts over the past 25 years. The origin of TRV is not understood, but present observations can be accommodated [2] within the standard model (SM). Although most nuclear physics experiments have not yet achieved sufficient accuracy to test the myriad of proposed extensions of the SM [3], the motivation for additional precision experiments is that the eventual observation of TRV outside of  $K$  meson decay may require the introduction of "new physics" and lead to an understanding of the origins of TRV in the SM.

Time-reversal invariance can be investigated with measurements of  $T$ -odd correlations in the beta decay of polarized nuclei. For our purposes the beta-decay transition rate can be written in terms of the nuclear polarization  $\mathbf{J}$  and the velocities  $\mathbf{v}$  (in units of  $c$ ) as [4]

$$W = W_0[1 + A\mathbf{v}_e \cdot \mathbf{J} + D\mathbf{J} \cdot (\mathbf{v}_e \times \mathbf{v}_\nu) + R\hat{\sigma}_e \cdot (\mathbf{J} \times \mathbf{v}_e)],$$

where  $A$  is the usual  $T$ -even parity-violating asymmetry parameter and  $\hat{\sigma}_e$  is the direction in which the electron polarization  $\mathbf{P} = R(\mathbf{J} \times \mathbf{v}_e)$  is measured. The  $P$ -even,  $T$ -odd electron-neutrino correlation parameter  $D$  is sensitive to a complex phase between the dominant vector and axial-vector ( $V-A$ ) currents. Experiments for the neutron and  $^{19}\text{Ne}$  give the limit [3]  $D < 10^{-3}$ . On the contrary, the  $P$ - and  $T$ -odd nuclear-electron polarization parameter  $R$  is sensitive to exotic scalar and tensor interaction terms, which are not present in the standard ( $V-A$ ) description of nuclear beta decay. Up to now,  $R$  has been measured only for  $^{19}\text{Ne}$ ; the measured value,  $R = -0.079 \pm 0.053$ , depends on both the imaginary parts of the scalar ( $C_S$ ) and of the tensor ( $C_T$ ) coupling constants. Assuming  $\text{Im}C_T = 0$ , one obtains a limit for the scalar interaction,  $\text{Im}(C_S + C_S')/C_A = 0.24 \pm 0.16$ , from

this experiment [5].

Here we report a measurement of  $R$  for the decay of  $^8\text{Li} \rightarrow ^8\text{Be}(2.9 \text{ MeV}) + e^- + \bar{\nu}_e$ . Since there is an isospin change ( $\Delta T = 1$ ) in this transition, the Fermi matrix element vanishes, and one has an essentially pure Gamow-Teller transition with  $\log_{10} t = 5.4$ , half-life  $t = 0.84 \text{ s}$ , end-point energy  $E_0 \approx 14 \text{ MeV}$ , and  $A = -\frac{1}{3}$ . Ignoring isospin impurities and final-state interactions, which can be neglected at the present level of accuracy, the largest contribution to  $R$  comes from an imaginary axial-vector-tensor interference term [4], viz.,

$$R = \frac{2}{3} \frac{\text{Im}(C_T C_A'^* + C_T' C_A^*)}{|C_A|^2 + |C_A'|^2} \approx \frac{\text{Im}(C_T + C_T')}{3C_A}.$$

Thus the interpretation of  $R$  for  $^8\text{Li}$  is simpler than in the case of  $^{19}\text{Ne}$ , since its value depends only on  $\text{Im}C_T$  and not on a combination of  $\text{Im}C_S$  and  $\text{Im}C_T$ . (The approximation is valid for  $C_A = C_A' = \text{real}$ .) Examples of mechanisms that could generate a charged weak tensor interaction are the exchange of spin-2 bosons or coupling to spin-0 leptoquarks [3].

The experiment was performed at the Paul Scherrer Institute with the apparatus shown schematically in Fig. 1. Polarized  $^8\text{Li}$  nuclei with average activity  $7 \times 10^8 \text{ Bq}$  were produced by the  $^7\text{Li}(d,p)^8\text{Li}$  reaction using a 0.4- $\mu\text{A}$ , 10-MeV deuteron beam whose vertical polarization  $p_y = \pm(0.48 \pm 0.01)$  was determined by  $d$ -C elastic scattering. The  $^8\text{Li}$  polarization  $J_y$  has the same sign as  $p_y$ . The target, a 5-mm-diam rod of 99.9% enriched  $^7\text{Li}$  metal, was cooled with liquid nitrogen and placed in an external field  $B_y = 5 \text{ mT}$  to obtain a long polarization relaxation time. The experiment was performed in a cyclic fashion, with a 0.33-s activation of the target followed by a measuring period divided into 24 intervals of 44 ms. The sign of  $p_y$  was reversed after four activation-measurement cycles. The nuclear polarization integrated over the measurement period,  $\langle J \rangle = 0.11 \pm 0.01$ , was deduced from the beta count rate in two small scintillator telescopes at angles  $\theta = 38^\circ$  and  $142^\circ$  with respect to the  $^8\text{Li}$  polarization direction. This measurement is in good agreement with the value calculated from the beam polarization  $p_y$  and the known (cf. Ref. [6]) polarization transfer coefficient  $K_y^{p'} = 0.21$  for a thick target numeri-

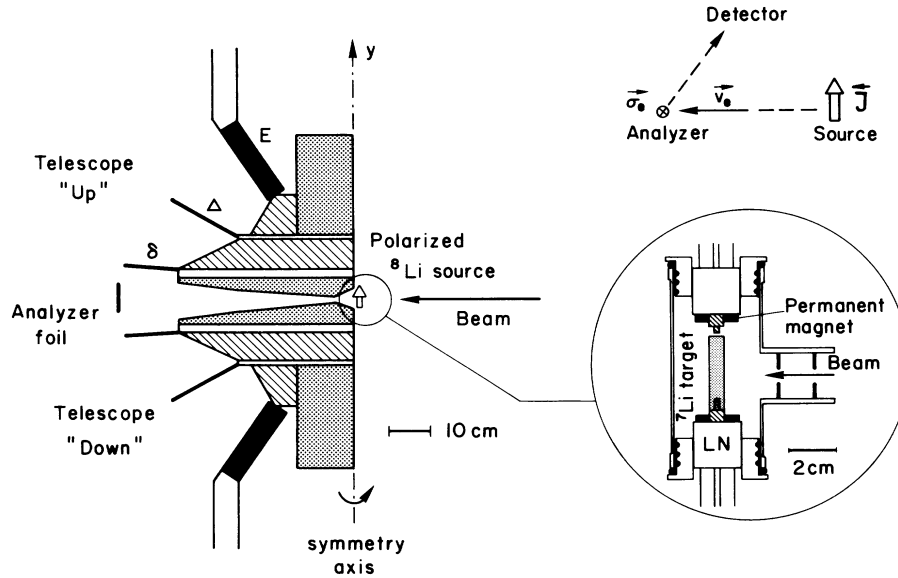


FIG. 1. On the left-hand side the main parts of the experimental setup are shown. The apparatus has  $180^\circ$  azimuthal symmetry about the vertical symmetry axis. Electrons emitted from  $^8\text{Li}$  source are scattered on the analyzer foil and measured in two triple scintillator telescopes ( $\delta$ ,  $\Delta$ , and  $E$  detectors). On the upper part of the right-hand side the vectors which enter into the definition of the  $R$  parameter are shown schematically. Inset: The target chamber with the permanent magnets for the magnetic holding field and the liquid-nitrogen (LN) cooling for the  $^7\text{Li}$  rod.

cally integrated over the cycle described above. The measured mean relaxation time of the polarization was constant during all data taking runs,  $T_1 = 3.6 \pm 0.1$  s. As a check of the cleanness of the source we measured the electron spectrum and compared it to the theoretical form of an allowed  $\beta$  transition [folding in the finite width of the final state ( $^8\text{Be}$ ,  $\Gamma = 1.5$  MeV) and the resolution of the scintillation detector, see Fig. 2(a)]. Furthermore, the number of emitted electrons with an energy larger than 3 MeV after chopping off the beam was measured; no other substantial activity is visible in the time spectra [see Fig. 2(c)].

As shown in Fig. 1, Mott scattering from a high- $Z$  foil located in the median plane into the scintillator telescopes (detectors  $\delta$ ,  $\Delta$ , and  $E$ ) placed above (up detector) and below (down detector) the median plane was used to measure the component of the electron polarization  $\mathcal{P}$  in the direction perpendicular to  $\mathbf{J}$  and  $\mathbf{v}_e$ . The expected rate in the up and down detectors is  $w_{u,d} = w_0[1 + \epsilon(\mathcal{P} \cdot \hat{n})]$ , where  $\epsilon$  is the Mott analyzing power [7] and  $\hat{n}$  is perpendicular to the Mott scattering plane. Since  $\mathcal{P} = R(\mathbf{J} \times \mathbf{v}_e)$  changes sign for nuclear polarization  $J_y = \pm J$ , defining the ratio

$$r = \left( \frac{w_u(J_y = +J)w_d(J_y = -J)}{w_u(J_y = -J)w_d(J_y = +J)} \right)^{1/2}$$

gives an asymmetry  $\mathcal{A}_R$ ,

$$\mathcal{A}_R = R \langle \epsilon \rangle \langle J \rangle = (r - 1)/(r + 1),$$

where  $\langle \epsilon \rangle$  is averaged over the beta energy spectrum and detector geometry (see below) and  $\langle J \rangle$  is averaged over time. Detector efficiencies, solid angles, and activity nor-

malizations cancel in the ratio  $r$ . Mott scattering in the geometry shown in Fig. 1 was selected for the electron polarization analyzer because  $\epsilon$  is relatively large ( $-0.25$  to  $-0.10$ ) over the range of energies (4–12 MeV) and scattering angles ( $120^\circ$  to  $155^\circ$ ) used in the experiment. Although the Mott cross section is small at these large angles, sufficiently high rates were achieved by constructing an apparatus with rotational ( $\phi$ ) symmetry about  $J_y$ .

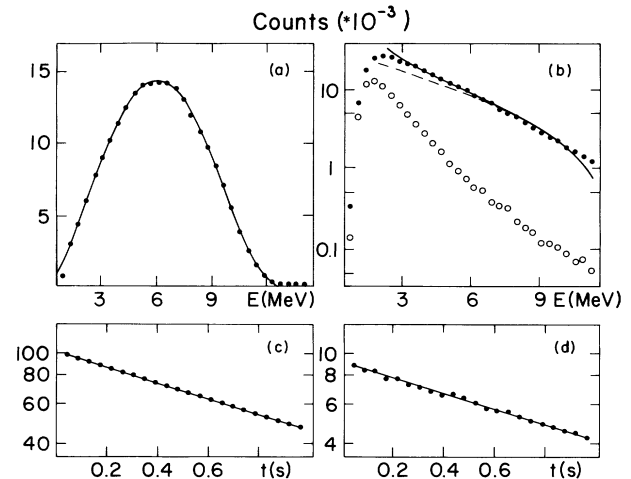


FIG. 2. Energy spectra and decay after activation of electrons from the Li source [(a) and (c), respectively], and of the Mott-scattered electrons detected in the  $\delta$ - $\Delta$ - $E$  telescopes of Fig. 1 [(b) and (d), respectively]. The open circles in (b) show the background measured with the Pb foil removed. The calculated energy spectra [curves in (a) and (b)] are explained in the text. The calculated exponential decays, which are shown in (c) and (d), are based on the known half-life of  $^8\text{Li}$  ( $t = 0.84$  s).

In principle the full  $\Delta\phi=360^\circ$  azimuthal angular range can be used. A preliminary experiment [8] employed an apparatus with  $\Delta\phi=90^\circ$ . For the results presented here, the  $h=7$  cm high,  $d=110$  cm diameter,  $35\text{-mg/cm}^2$  Pb scattering foil and the 2-mm-thick transmission  $\delta$  and  $\Delta$  and 4-cm-thick  $E$  plastic scintillator detectors subtended  $\Delta\phi=180^\circ$ . In the design of the apparatus the reduction of background due to electrons (or their associated bremsstrahlung) which are not scattered in the analyzer foil was of paramount importance and led, after many tests, to the shielding arrangement shown in Fig. 1. This background is expected to have an anisotropy since the electron angular distribution  $W(\theta)=W_0(1+Av_eJ_y\cos\theta)$  is modulated by polarization reversal. About one-third of the measuring time was devoted to periodic measurements with the scattering foil removed. A summed  $\delta$ ,  $\Delta$ , and  $E$  detector foil-in minus foil-out (REAL) pulse height spectrum is shown as solid circles in Fig. 2(b). The foil-out background contribution, shown as open circles, is about 8% of the total number of counts for  $E_e > 4$  MeV. The asymmetry [as defined above,  $\mathcal{A}_{\text{back}}=(r-1)/(r+1)$ ] of the background contribution, averaged over all measurements, was  $\mathcal{A}_{\text{back}}=(1.9\pm 1.0)\times 10^{-3}$ . Figure 2(d) shows the time decay over the measurement period of the REAL spectrum for  $E_e > 4$  MeV. The solid line is an exponential fit which gives  $t=0.84\pm 0.01$  s, in excellent agreement with the  $^8\text{Li}$  half-life. There is no detectable contribution from activities other than  $^8\text{Li}$  in the REAL spectrum for  $E_e > 4$  MeV.

A Monte Carlo calculation of the electron spectrum integrated over the scattering foil, detector array solid angle, and detector resolution for a single Mott scattering in the Pb foil only is shown as the dashed curve in Fig. 2(b). The solid curve shows a calculation which includes multiple scattering [9] in the Pb foil and  $\delta$  detectors and plural scattering in the Pb foil for the same integrated  $^8\text{Li}$  activity. For the two calculations shown in Fig. 2, we obtain the analyzing powers  $\langle\epsilon\rangle=-0.12$  and  $-0.10$ , respectively, with an uncertainty of about  $\pm 10\%$ . (The reduction to  $\langle\epsilon\rangle=-0.12$  arises primarily from the angular averaging of  $\mathcal{P}\cdot\hat{n}$  over the detector solid angle.) We use the value  $\langle\epsilon\rangle=-0.10\pm 0.01$ , where the uncertainty is treated as a systematic error, for the analysis presented below.

We verified the accuracy of the multiple-scattering correction by performing corresponding Monte Carlo calculations for the very precise  $^{32}\text{P}$  electron polarization measurements of Brosi *et al.* [10]. At 616 keV and for a Au scattering foil  $2.21\text{ mg/cm}^2$  thick, which provides a multiple-scattering angular distribution similar to the present experiment, Brosi *et al.* measure an asymmetry  $\mathcal{A}_{\text{expt}}=0.195\pm 0.003$ . Our calculation gives  $\mathcal{A}_{\text{MC}}=0.186$ . For the nine measurements for Au foil thicknesses between  $0.44$  and  $6.27\text{ mg/cm}^2$ , corresponding to measured asymmetries  $\mathcal{A}_{\text{expt}}$  between  $0.304$  and  $0.093$ , we obtain excellent agreement with  $\mathcal{A}_{\text{MC}}/\mathcal{A}_{\text{expt}}=1.02\pm 0.05$ . Additional calculations showed that depo-

larization of electrons in the Li source was  $<0.002$ , and that the net transverse polarization components induced by scattering in the target and in the shielding was  $<0.003$ . These contributions are negligible at the present level of accuracy.

Although constant or slowly varying backgrounds pose no special problems, corrections must be applied for all effects which lead to changes in polarimeter detector rates coherent with spin reversal. By far the largest effect of this type is the false asymmetry  $\mathcal{A}_{a\Omega}$  due to the nonuniform illumination ( $I$ ) of the scattering foil. The electron angular distribution  $W(\theta)$  gives

$$I(\alpha, J_y = \pm J) = I_0(1 \pm Av_e J \sin\alpha) \approx I_0(1 \pm Av_e J \alpha),$$

where  $\alpha=\pi/2-\theta$ . Integrating the rate  $w_{u,d}(J_y = \pm J)$  in the Mott detectors over the foil with this illumination gives the approximate result for this false asymmetry

$$\mathcal{A}_{a\Omega} = \frac{1}{3} A \langle J \rangle \rho \alpha_0^2,$$

where

$$\rho = \frac{1}{\langle \sigma_M \Omega \rangle} \frac{\partial \langle \sigma_M \Omega \rangle}{\partial \alpha},$$

$\alpha_0=h/d$  is the polar angle subtended by the foil, and  $\sigma_M$  is the Mott cross section. We measured  $\rho=3.0\pm 0.4$  using a  $h=1$  cm foil displaced from the median plane. The Monte Carlo calculation with multiple and plural scattering gives  $\rho=2.6\pm 0.1$ . The measured value was used to compute the correction given in Table I.

Two smaller corrections come from the accidental events, which were directly measured, and from gain shifts in the Mott detectors. The count rates in the detectors are about 2 orders of magnitude higher during activation than during the measuring period, and decrease by more than a factor of 2 over this period. Using stabilized light-emitting diodes we measured an approximately 5% decrease in the scintillator photomultiplier gain over the measuring period. The residual false asymmetry and uncertainty from this gain shift,  $\mathcal{A}_{\text{gain}}=(-1\pm 2)\times 10^{-5}$  with threshold corrections applied in a subsequent off-line analysis, is much smaller than might be naively expected because only the difference in gain shift coherent with spin reversal contributes to the false asymmetry.

The results of the preliminary measurement [11] and those of the present investigation, in which 28 runs, each with a duration of 60 min, have been evaluated, are given in Table I. The weighted mean of the foil-in (no background subtraction) asymmetries for a threshold  $E_e=4$  MeV is  $(9\pm 12)\times 10^{-5}$ . The background subtraction and other corrections are also given in the table. Our result,  $R=(7\pm 15)\times 10^{-3}$ , depends only slightly on the  $E_e$  threshold (for a higher threshold the statistical error is larger, while for a lower threshold the background and uncertainty in  $\langle\epsilon\rangle$  are larger) and shows no systematic trends ( $\chi^2/N_{\text{DF}}\approx 1.0$  for all data subsets). Taking the two measurements together and including the uncertainty in the target polarization,  $\langle J \rangle=0.11\pm 0.01$ , and the Mott

TABLE I. Summary of experimental results: Raw data for the  $R$  coefficient and corrections to  $R$  (all values in units of  $10^{-3}$ ). The errors include all statistical and systematic contributions apart from common normalization factors (see text).

Value	Preliminary experiment	Present investigation
Raw data	$12 \pm 34$	$9 \pm 12$
Background	$-39 \pm 26$	$-13 \pm 8$
$\alpha\Omega$ effect	$11 \pm 5$	$13 \pm 2$
Gain shifts	$-1 \pm 3$	$-1 \pm 2$
Accidentals	$-7 \pm 8$	$-1 \pm 2$
Result	$-24 \pm 44$	$7 \pm 15$

analyzing power,  $\langle\epsilon\rangle = -0.10 \pm 0.01$ , we obtain as a final result

$$R = (4 \pm 14) \times 10^{-3}.$$

This is the most precise measurement of this  $T$ -odd correlation.

As a result of the low charge number ( $Z$ ) of the final nucleus and due to the high energy of the detected electrons, final-state interaction corrections [12] are extremely small for  ${}^8\text{Li}$ ,

$$R_{\text{FSI}} \approx \frac{1}{3} \frac{Z\alpha m_e}{p_e} < 0.001 \text{ for } E_e > 4 \text{ MeV},$$

and can be neglected at the present level of accuracy. Corrections for weak magnetism and other recoil-order terms are 5 times smaller yet.

The result is consistent with no time-reversal violation. It provides a new ( $1\sigma$ ) limit on imaginary tensor couplings in semileptonic strangeness-conserving weak decays,

$$-0.03 < \frac{\text{Im}(C_T + C_T')}{C_A} < 0.05.$$

The only earlier limit on  $\text{Im}(C_T + C_T')/C_A = -0.04 \pm 0.03$  has been derived by Skalsey and Hatamian [13] from small final-state corrections to longitudinal electron polarizations. The main input into their analysis is the precise measurements of Van Klinken [14] on the decay of  ${}^{153}\text{Sm}$ . The final value for  $\text{Im}(C_T + C_T')$ , however, depends critically on some assumptions which had to be

made in the evaluation of that experiment (only allowed transitions, pure Gamow-Teller decays) and various constraints on the values of other coupling constants.

In conclusion, our  $R$  coefficient measurement provides the first direct test of time-reversal violation induced by charged tensor couplings in nuclear beta decay. In the future we plan to construct an apparatus which utilizes the full  $\Delta\phi = 360^\circ$  symmetry and, with somewhat longer run times, obtain a statistical error in  $R$  well below 0.01. At this level of precision systematic uncertainties and final-state corrections [12] will have to be carefully evaluated.

This work was supported in part by the Swiss National Foundation and the U.S. National Science Foundation Grant No. PHY-9019983.

- 
- [1] C. N. Yang and T. D. Lee, *Phys. Rev.* **104**, 254 (1956).
  - [2] See, e.g., Particle Data Group, J. J. Hernández *et al.*, *Phys. Lett. B* **239**, 1 (1990). Since  $PCT$  conservation has been tested to a very high precision,  $T$  and  $PC$  violation here are regarded as equivalent.
  - [3] P. Herczeg, in *Fundamental Symmetries in Nuclei and Particles*, edited by H. Henrikson and P. Vogel (World Scientific, Singapore, 1989), p. 47.
  - [4] J. D. Jackson, S. B. Treiman, and H. W. Wyld, *Nucl. Phys.* **4**, 206 (1957).
  - [5] M. B. Schneider, F. P. Calaprice, A. L. Hallin, D. W. MacArthur, and D. F. Schreiber, *Phys. Rev. Lett.* **51**, 1239 (1983). We always use the ratios of exotic coupling constants to the dominant regular ones. In this way different analyses and experiments can be compared directly.
  - [6] Z. Wang, R. A. Bigelow, P. A. Quin, and J. R. Liechti, *Phys. Rev. C* **40**, 1586 (1989).
  - [7] N. Sherman, *Phys. Rev.* **103**, 1601 (1956).
  - [8] H. Lüscher, Ph.D. thesis, Eidgenössische Technische Hochschule Zürich, 1991.
  - [9] H. Wegener, *Z. Phys.* **151**, 252 (1958).
  - [10] A. R. Brosi *et al.*, *Nucl. Phys.* **33**, 353 (1962).
  - [11] J. Sromicki *et al.*, *J. Phys. (Paris)*, Colloq. **51**, C6-527 (1990).
  - [12] P. Vogel and B. Werner, *Nucl. Phys.* **A404**, 345 (1983).
  - [13] M. Skalsey and M. S. Hatamian, *Phys. Rev. C* **31**, 2218 (1985).
  - [14] J. Van Klinken, *Nucl. Phys.* **75**, 145 (1966).

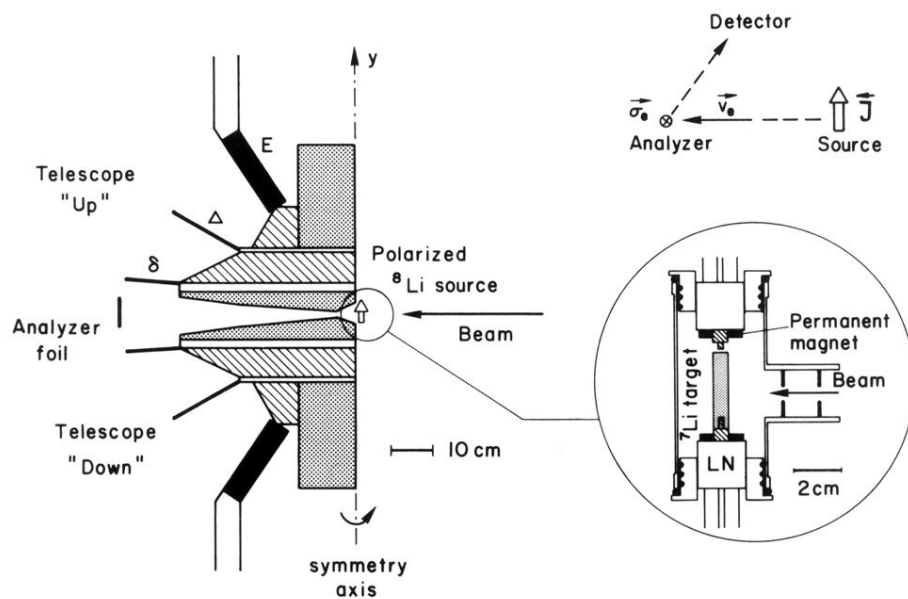


FIG. 1. On the left-hand side the main parts of the experimental setup are shown. The apparatus has  $180^\circ$  azimuthal symmetry about the vertical symmetry axis. Electrons emitted from  $^8\text{Li}$  source are scattered on the analyzer foil and measured in two triple scintillator telescopes ( $\delta$ ,  $\Delta$ , and  $E$  detectors). On the upper part of the right-hand side the vectors which enter into the definition of the  $R$  parameter are shown schematically. Inset: The target chamber with the permanent magnets for the magnetic holding field and the liquid-nitrogen (LN) cooling for the  $^7\text{Li}$  rod.